Modeling heat and mass transfer in laminar forced convection in a vertical channel: influence of Reynolds number

ABSTRACT

This work concerns a numerical study of heat and mass transfer in laminar forced convection in a vertical channel. Based on simplifying assumptions, the flow was modeled by the Navier-Stokes equations and the flow conservation equation. The finite volume method was used to discretize the equations, and the resulting systems of algebraic equations were solved using Thomas and Gauss algorithms. The main focus was on the influence of Reynolds number on heat and mass transfer. Results presented in the form of isotherms, iso-concentrations, Sherwood and Nusselt numbers show that the Reynolds number plays an important role in heat and mass transfer in a vertical channel.

Keywords: Laminar forced convection, heat and mass transfer, Reynolds number, vertical channel.

1. INTRODUCTION

The interest in studying convection in channels is dictated by its importance in applications such as smoke-drying, building heating, cooling of electronic components, thermal desalination of sea water [1][2][3]. Several parameters, such as the nature of the fluid, its velocity, relative humidity, inlet temperature, and the temperature of the walls, make channel flow complex. They have therefore been the subject of numerous studies, both numerical and experimental. O. Mechergui[2], who studied the phenomenon of evaporation in laminar flow in his thesis, demonstrated the influence of parameters such as wall temperature, heat flux density, temperature and humidity at the channel inlet on the velocity, concentration and temperature profiles inside the channel for heat and masstransfer. To demonstrate the dependence of the physical properties of moist air on both temperature and water vapor concentration, Oulaid*et al.*[4]considered a warm air stream whose physical properties are initially constant, and then variable. As the difference between the results of the two models was significant (between 8 and 30%) for all hydrodynamic, thermal and mass quantities, they concluded that it was important to consider the variability of thermo-physical properties in the mathematical model. Given the importance of parameters such as velocity, temperature and humidity, some authors have focused on their effects on heat and mass transfer. For example, Boukadida*et al.*[5]studied the effect of control parameters on air velocity, temperature and humidity inside a horizontal channel. Their results showed that air temperature, longitudinal velocity and water vapor concentration increased from the inlet to the outlet of the channel. Helel *et al.*[6]revealed, after a numerical study of heat and mass transfer mechanisms in laminar flow, that these transfers are greater in the vicinity of the leading edge than at the outlet. A numerical study carried out by N. Galanis *et al.*[7]on mixed laminar convection with phase change between two parallel flat plates wetted with a liquid film of water at a constant temperature lower than that of air at the channel inlet, revealed that the ratio between the latent and sensible Nusselt number is seven at the channel inlet,

whereas it is three at the outlet. Inside the channel, Lin *et al.*[8], who studied the combined effects of buoyancy, thermal and mass diffusion on heat transfer by laminar forced convection, showed that heat transfer in the flow is dominated by latent mode transport, with the ratio of latent to sensible heat flux having a minimum for a fixed parietal temperature. The effect of flow velocity on heat transfer has been studied by Yan *et al.*[9]**.** In a typical study of coupled heat and mass transfer along a heated plate, in addition to the importance of latent heat transport, the authors showed that parietal temperature decreases with increasing flow velocity. Mezaache and Daguenet [10] have numerically examined the evaporation, in a forced flow of humid air, of a thin film of water trickling over an inclined flat plate, considered adiabatic or traversed by a constant heat flux. They have shown that the effect of flow velocity is an important parameter, and that heat transfer is dominated by that associated with the liquid-vapor transition. Cherif *et al.*[11][12]presented the results of an experimental and numericalstudy of coupledheat and mass transfer in a vertical channel. Evaporated mass flux and thermal efficiency are calculated for different heat flux densities and flow velocities. They revealed that evaporation takes place over the majority of the wall surface and, in some cases, evaporative cooling occurs particularly for low heat flux and high air velocities. Turki *et al*. [13]have shown that the contribution of forced convection to heat transfer is greater than that of mixed convection. The results of the literature show that the influence of Reynolds number on heat and mass transfer has not been sufficiently investigated, hence the interest of the present work, which looks at a global visualization of the flow through iso-values.

2. METHODOLOGY

2.1. DESCRIPTION OF THE PHYSICS MODEL

A fluid of temperature T_e and relative humidity $\phi_e$enters a vertical channel with velocity U_e. The walls of the channel, of height H, are wet and separated by a distance 2R, R being the radius of the channel. The walls undergo evaporation of water vapor. Figure 1 shows the physical model of the channel studied.

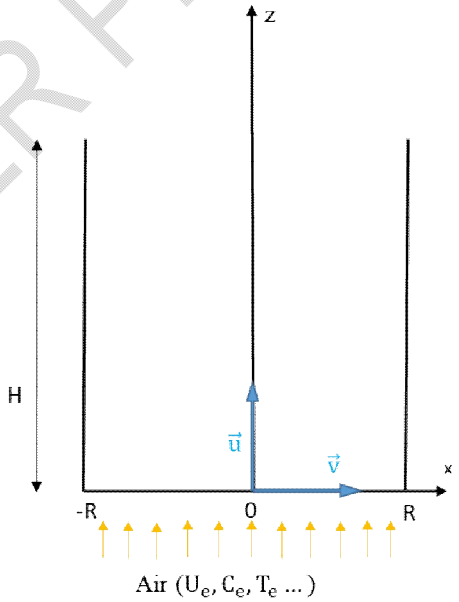

Fig. 1. The physical model

2.2. MATHEMATICAL FORMULATION

2.2.1. SIMPLIFYING HYPOTHESES

The hypotheses formulated are:

- The gaseous effluent is laminar, incompressible and Newtonian;
- Transfers are two-dimensional and take place in a forced laminar and unsteady regime;
- The Dufour and Soret effects are neglected;
- The radial driving pressure gradient is neglected;
- The condition of non-slip of the fluid on the walls is considered;
- The flow is rotationally symmetrical around the vertical axis (OZ), which restricts the study on the half channel.

2.2.2. TRANSFER EQUATIONS

Based on the above assumptions, the equations governing heat and mass transfer in the channel are the Navier-Stokes equations in addition to the flow conservation equation [14][15].The thermo-physical properties of air depend on temperature and humidity. Their calculations are detailed in the work of Feddaoui*et al*[16].

❖ **The continuityequation**

$$\frac{\partial(\rho V)}{\partial x} + \frac{\partial(\rho U)}{\partial z} = 0 \quad (1)$$

❖ **The axial equation of momentum**

$$\rho\frac{\partial U}{\partial t} + \frac{\partial(\rho VU)}{\partial x} + \frac{\partial(\rho UU)}{\partial z} = -\frac{\partial P}{\partial z} + \frac{\partial}{\partial x}\left(\mu\frac{\partial U}{\partial x}\right) + \frac{\partial}{\partial z}\left(\mu\frac{\partial U}{\partial z}\right) \quad (2)$$

❖ **The radial equation of momentum**

$$\rho\frac{\partial V}{\partial t} + \frac{\partial(\rho VV)}{\partial x} + \frac{\partial(\rho UV)}{\partial z} = \frac{\partial}{\partial x}\left(\mu\frac{\partial V}{\partial x}\right) + \frac{\partial}{\partial z}\left(\mu\frac{\partial V}{\partial z}\right) \quad (3)$$

❖ **The energy conservation equation**

$$\rho C_p\frac{\partial T}{\partial t} + \frac{\partial(\rho C_p VT)}{\partial x} + \frac{\partial(\rho C_p UT)}{\partial z} = \frac{\partial}{\partial x}\left(\lambda\frac{\partial T}{\partial x}\right) + \frac{\partial}{\partial z}\left(\lambda\frac{\partial T}{\partial z}\right) \quad (4)$$

❖ **The water vapor diffusion equation**

$$\rho\frac{\partial C}{\partial t} + \frac{\partial(\rho VC)}{\partial x} + \frac{\partial(\rho UC)}{\partial z} = \frac{\partial}{\partial x}\left(\rho D\frac{\partial C}{\partial x}\right) + \frac{\partial}{\partial z}\left(\rho D\frac{\partial C}{\partial z}\right) \quad (5)$$

❖ **The flow rate conservation equation**

$$\int_0^R Udx = Q_{ev} + Q_e \quad (6)$$

2.2.3. INITIAL CONDITIONS

$$U(x,z) = 0\ ;\ V(x,z) = 0\ ;\ C(x,z) = C_e;\ T(x,z) = T_e \quad (7a\text{-}d)$$

2.2.4. BOUNDARY CONDITIONS

- At the channel entrance: $z = 0; 0 \leq x \leq R$

$$U(x,z) = \frac{3}{2}U_e\left[1-\left(\frac{x}{R}\right)^2\right] \quad (8)$$

$$V(x,z) = 0\ ; C(x,z) = C_e;\ T(x,z) = T_e \quad (9a\text{-}c)$$

- At the channel outlet: $z = H; 0 \leq x \leq R$

$$\frac{\partial U(x,z)}{\partial z} = 0\ ;\ \frac{\partial V(x,z)}{\partial z} = 0\ ;\ \frac{\partial T(x,z)}{\partial z} = 0\ ;\ \frac{\partial C(x,z)}{\partial z} = 0 \quad (10a\text{-}d)$$

- At the axis of symmetry: $x = 0; 0 \leq z \leq H$

$$V(x,z) = 0 \quad (11)$$

$$\frac{\partial U(x,z)}{\partial x} = 0\ ;\ \frac{\partial T(x,z)}{\partial x} = 0\ ;\ \frac{\partial C(x,z)}{\partial x} = 0 \quad (12a\text{-}c)$$

- To the wall: $x = R; 0 \leq z \leq H$

$$U(x,z) = 0 \quad (13)$$

$$V(x,z) = V_{ev} \quad (14)$$

V_{ev}: is the evaporation rate at the wall. Its calculation is detailed in the work of Eckert *et al*. [17]. Its expression is:

$$V_{ev} = -\frac{D}{(1-C_P)}\frac{\partial C}{\partial x}\Big|_P \quad (15)$$

The mass fraction of water vapor corresponds to the saturation conditions explained by Dalton's law:

$$C_P = \frac{P_P M_V}{[P_P M_V + (P-P_P)M_a]} \quad (16)$$

$$-\lambda\left(\frac{\partial T}{\partial x}\right) - \rho L_V V_{ev} = -\lambda_s\left(\frac{T_{Pe}-T_{Pi}}{E}\right) = (h_R + h_C)(T_{amb} - T_{Pe}) \quad (17)$$

The convective transfer coefficient h_C is correlated with the Rayleigh number (GrPr) according to J. F Sacadura [18]:

$$h_C = Nu\lambda_{air}/H \quad (18)$$

$$Nu = a(GrPr)^m \quad (19)$$

For: $10^4 < GrPr < 10^9$; $a = 0.59$; $m = 0.25$ (20)

For: $10^9 < GrPr < 10^{13}$; $a = 0.21$; $m = 0.4$ (21)

$$Gr = \frac{g\beta_T(T_{Pe}-T_{amb})H^3}{\vartheta_{air}^2} \quad (22)$$

$$h_R = \gamma\sigma(T_{Pe}^2 + T_{amb}^2)(T_{Pe} + T_{amb}) \quad (23)$$

The total heat flux exchanged between the wet wall and the flow is the sum of the sensible heat flux and the latent heat flux.

$Q_T = Q_S + Q_L = \lambda \frac{\partial T}{\partial x}\Big|_P + \dot{m}_C'' L_V$ (24)

$Nu_S = \frac{Dh}{\lambda}\frac{Q_S}{(T_P - T_b)} = \frac{Dh}{(T_P - T_b)}\frac{\partial T}{\partial x}\Big|_P$ (25)

$Nu_L = \frac{Dh}{\lambda}\frac{Q_L}{(T_P - T_b)} = \frac{\dot{m}_C'' L_V Dh}{\lambda(T_P - T_b)}$ (26)

$Sh = \frac{Dh}{(C_P - C_b)}\frac{\partial C}{\partial x}\Big|_P$ (27)

$Re = UeDh/\vartheta e$ (28)

$Dh = 2R$ (29)

$\mathrm{Pr} = \rho_e \vartheta_e C_{Pe}/\lambda_e$ (30)

$Sc = \vartheta_e/D_e$ (31)

2.2.5. DIMENSIONLESS EQUATIONS

The dimensionless equations and boundary conditionsare obtained by dividing the various variables by thevariables by the characteristic quantities of the system given in table 1.

Table. 1.Dimensionless variables

Designation	Dimensionless variable
Radial coordinate	$x^\star = \frac{x}{Dh}$
Axial coordinate	$x^\star = \frac{x}{Dh}$
Radial velocity	$V^\star = \frac{V}{U_e}$
Temperature	$T^\star = \frac{T}{T_e}$
Pressure	$P^\star = \frac{P}{\rho_e U_e^2}$
Concentration	$C^\star = \frac{C}{C_e}$
Density	$\rho^\star = \frac{\rho}{\rho_e}$
Dynamic viscosity	$\vartheta^\star = \frac{\vartheta}{\vartheta_e}$
Thermal conductivity	$\lambda^\star = \frac{\lambda}{\lambda_e}$
Thermal diffusivity	$D^\star = \frac{D}{D_e}$
Specific heat	$Cp^\star = \frac{Cp}{Cp_e}$
Radius of channel	$R^\star = \frac{R}{Dh}$
Height of channel	$H^\star = \frac{H}{Dh}$
kinematic viscosity	$\boldsymbol{\mu}^\star = \frac{\boldsymbol{\mu}}{\boldsymbol{\mu_e}}$

- **The continuityequation**

$$\frac{\partial(\rho^* V^*)}{\partial x^*} + \frac{\partial(\rho^* U^*)}{\partial z^*} = 0 \qquad (32)$$

- **The axial equation of momentum**

$$\rho^* \frac{\partial U^*}{\partial \tau} + \frac{\partial(\rho^* V^* U^*)}{\partial x^*} + \frac{\partial(\rho^* U^* U^*)}{\partial z^*} = -\frac{\partial P^*}{\partial z^*} + \frac{\partial}{\partial x^*}\left(\frac{\mu^*}{Re}\frac{\partial U^*}{\partial x^*}\right) + \frac{\partial}{\partial z^*}\left(\frac{\mu^*}{Re}\frac{\partial U^*}{\partial z^*}\right) \quad (33)$$

- **The radial equation of momentum**

$$\rho^* \frac{\partial V^*}{\partial \tau} + \frac{\partial(\rho^* V^* V^*)}{\partial x^*} + \frac{\partial(\rho^* U^* V^*)}{\partial z^*} = \frac{\partial}{\partial x^*}\left(\frac{\mu^*}{Re}\frac{\partial V^*}{\partial x^*}\right) + \frac{\partial}{\partial z^*}\left(\frac{\mu^*}{Re}\frac{\partial V^*}{\partial z^*}\right) \qquad (34)$$

- **The energy conservation equation**

$$\rho^* C_P^* \frac{\partial T^*}{\partial \tau} + \frac{\partial(\rho^* C_P^* V^* T^*)}{\partial x^*} + \frac{\partial(\rho^* C_P^* U^* T^*)}{\partial z^*} = \frac{1}{PrRe} \quad (35)$$

- **The water vapor diffusion equation**

$$\rho^* \frac{\partial C^*}{\partial \tau} + \frac{\partial(\rho^* V^* C^*)}{\partial x^*} + \frac{\partial(\rho^* U^* C^*)}{\partial z^*} = \frac{1}{ScRe}\left[\frac{\partial}{\partial x^*}\left(\rho^* D^* \frac{\partial C^*}{\partial x^*}\right) + \frac{\partial}{\partial z^*}\left(\rho^* D^* \frac{\partial C^*}{\partial z^*}\right)\right] \quad (36)$$

- **The flow rate conservation equation**

$$\int_0^{R^*} U^* dx^* = Q_{ev}^* + Q_e^* \quad (37)$$

2.2.6. INITIAL CONDITIONS

$$U^*(x^*, z^*) = 0\,;\; V^*(x^*, z^*) = 0\,;\; T^*(x^*, z^*) = 1\,;\; C^*(x^*, z^*) = 1 \qquad (38a\text{-}d)$$

2.2.7. BOUNDARY CONDITIONS

- At the channel entrance; $z^* = 0\,; 0 \le x^* \le R^*$

$$U^*(x^*, z^*) = \frac{3}{2}\left[1 - \left(\frac{x^*}{R^*}\right)^2\right] \qquad (39)$$

$$V^*(x^*, z^*) = 0\,;\; T^*(x^*, z^*) = 1\,;\; C^*(x^*, z^*) = 1 \qquad (40a\text{-}c)$$

- To the wall: $x^* = R^*\,; 0 \le z^* \le H^*$

$$U^*(x^*, z^*) = 0\,;\; V^*(x^*, z^*) = V_{ev}^* \quad (41)$$

$$V_{ev}^* = \frac{D}{DhU_e\left(1/C_e - C_p^*\right)}\left.\frac{\partial C^*}{\partial x^*}\right|_P \quad (42)$$

$$C_p^* = \frac{P_P^* - M_v^*}{P_P^* M_v^* + (P^* - P_P^*)M_a^*} \qquad (43)$$

$$\lambda^*\left(\frac{\partial T^*}{\partial x^*}\right) + \frac{\rho^* L_V V_{ev} Dh}{\lambda_e T_e} = \lambda_S^*\left(\frac{T_{Pi}^* - T_{Pe}^*}{E^*}\right) = \frac{Dh}{\lambda_0}(h_R + h_C)(T_{Pe}^* - T_{amb}^*) \qquad (44)$$

- At the axis of symmetry: $x^* = 0\,; 0 \le z^* \le H^*$

$$\partial V^*(x^*, z^*) = 0 \qquad (45)$$

$$\frac{\partial U^*(x^*,z^*)}{\partial x^*} = 0\,;\; \frac{\partial T^*(x^*,z^*)}{\partial x^*} = 0\,;\; \frac{\partial C^*(x^*,z^*)}{\partial x^*} = 0 \qquad (46a\text{-}c)$$

- At the channel outlet: $z^* = H^*$; $0 \leq x^* \leq R^*$

$$\frac{\partial U^*(x^*,z^*)}{\partial z^*} = 0 \; ; \; \frac{\partial V^*(x^*,z^*)}{\partial z^*} = 0 \; ; \; \frac{\partial T^*(x^*,z^*)}{\partial z^*} = 0 \; ; \; \frac{\partial C^*(x^*,z^*)}{\partial z^*} = 0 \qquad (47a\text{-}d)$$

The Nusselt and Sherwood numbers become:

$$Nu_S = \frac{1}{(T_P^* - T_b^*)} \frac{\partial T^*}{\partial x^*}\Big|_p \qquad (48)$$

$$Nu_L = \frac{\dot{m}_C'' L_V D h}{\lambda_e \lambda^* T_e (T_P^* - T_b^*)} \qquad (49)$$

$$Sh = \frac{1}{(C_P^* - C_b^*)} \frac{\partial C^*}{\partial x^*}\Big|_p \qquad (50)$$

2.3. NUMERICAL METHODOLOGY

The discretization of equations (32), (34), (35) and (36) by the finite volume method [17] leads to an algebraic equation system of N equations with N unknowns. Each equation system obtained is tridiagonal and is therefore solved by Thomas' algorithm. As for equation (33), it leads to a system of N equations with (N+1) unknowns. For this, it is completed by equation (37) and then solved by the Gauss algorithm. The convergence criterion chosen is:

$$\frac{\Phi^{k+1}(I,J) - \Phi^k(I,J)}{\Phi^{k+1}(I,J)} < 10^{-5} \qquad (51)$$

In this expression, k represents the number of iterations and $\boldsymbol{\Phi}$ =*T*, C*, U*, V*.*

3. RESULTS AND DISCUSSION

The results are recorded when the regime stabilizes at a time t = 3500s and are presented in tabular, profile and iso-values form under the followingconditions:T_{amb}=298.15K, T_e=323.15K with Reynolds number between 500 and 1500.

3.1.MODEL VALIDATION

To validate our numerical calculation code, we compared our numerical results with those of Othmane [19], for a thermally developing flow with mass transfer(see fig 2). The relative error resulting from comparison of the two results is of the order of 7%.

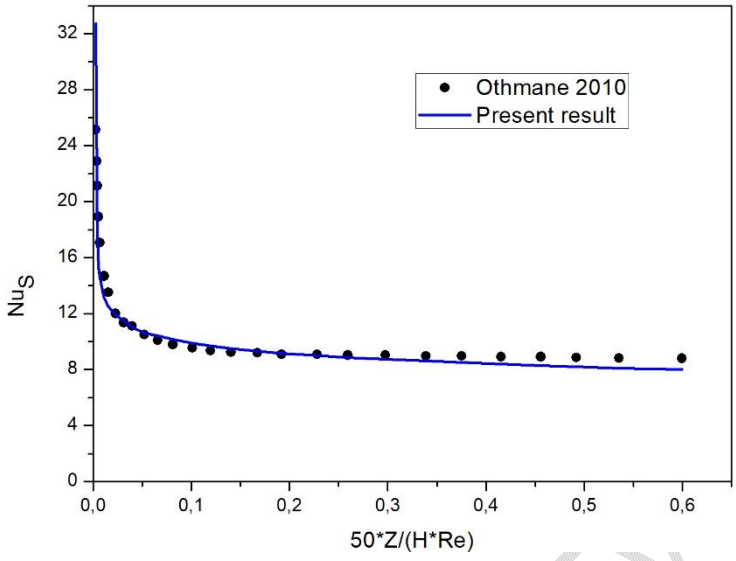

Fig. 2. Validation of the numerical code (To = 20˚C, Tw = 40˚C, ϕo = 50%, Pr= 0.703, Sc = 0.592, Re = 400).

3.2.MESH SENSITIVITY STUDY

To ensure that our results are independent of the mesh, a mesh sensitivity study was carried out. This study showed that the mesh size (41x112), even quadrupled, did not significantly modify the sensitive Nusselt (see table 2). Consequently, the mesh (41x112) was retained for the rest of the study.

Table. 2.Grid independence

Grid(X*,Z*)	Z*=20	Z*=40	Z*=60	Z*=80
		Values of Nu_S		
(41x112)	8,0186	6,5718	5,9367	5,5652
(82x224)	8,7732	6,8555	5,9899	5,4705

3.3. INFLUENCE OF REYNOLDS NUMBER ON THE DYNAMIC FLOW FIELD

Figures (3-5) show the distribution of the flow velocity field for Reynolds numbers of 500, 1000 and 1500 respectively.Laminar flow is observed for all three Reynolds numbers. The figures above provide an overall visualization of the flow velocity gradient, revealing higher velocities at the center of the channel and lower velocities near the walls. Flow velocity increases with Reynolds number, resulting in improved convective transfer. Indeed, the increase in inertial forces contributes to the thinning of the boundary layer, and hence to a reduction in diffusive momentum transport. This reduction is also accompanied by a reduction in fluid adhesion to the wall.

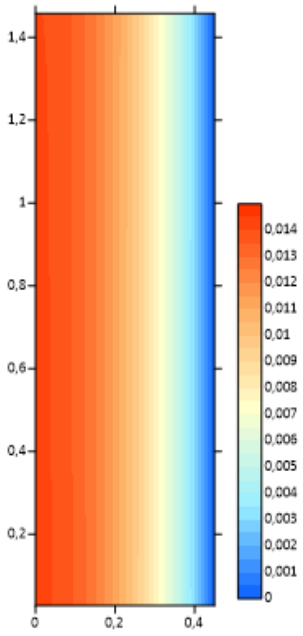

Fig.3. Velocity field, Re=500

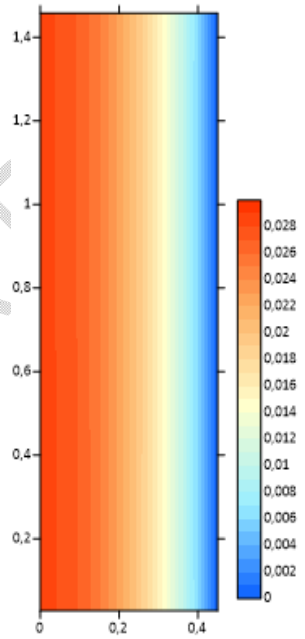

Fig.4. Velocityfield, Re=1000

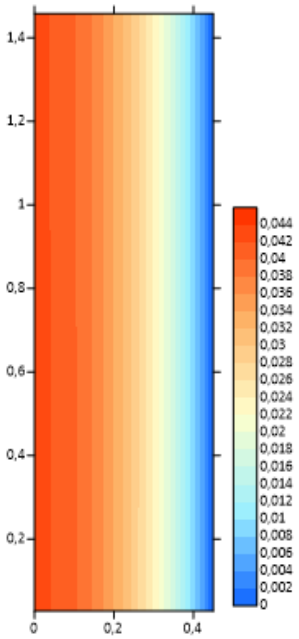

Fig.5. Velocityfield, Re=1500

3.4. INFLUENCE OF REYNOLDS NUMBER ON THE THERMAL FIELD

Figure 6 shows the thermal field distribution for a creeping flow with a Reynolds number of 10^{-3}.The thermal field is uniformly distributed. The isothermal lines are parallel to each other and to the direction of flow. Compared to the walls, the temperature gradients show higher values at the center of the channel. As the inertia of the flow decreases, viscous forces increase and diffusive momentum is transported. As a result, convective transfers are largely dominated by diffusive ones.

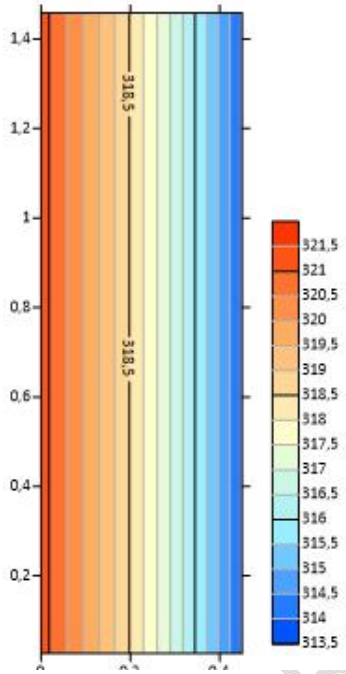

Fig.6. Thermal field for creep flow, Re=10^{-3}

Figures (7-9) show thermal field for Reynolds numbers ranging from 500 to 1500. The contours of the isotherms show a profile of thermal gradients, with higher temperatures in the center of the channel. The isothermal lines narrow near the walls, indicating a zone of strong thermal gradients. Increased inertial forces enhance convective momentum transport. This in turn reduces the fluid's adhesion to the wall, and hence diffusive transfer. As the Reynolds number increases, convective transfers improve and the boundary layer becomes thinner.

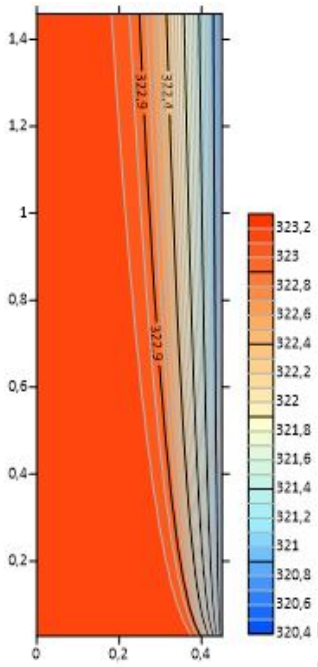

Fig.7. Thermal field, Re = 500

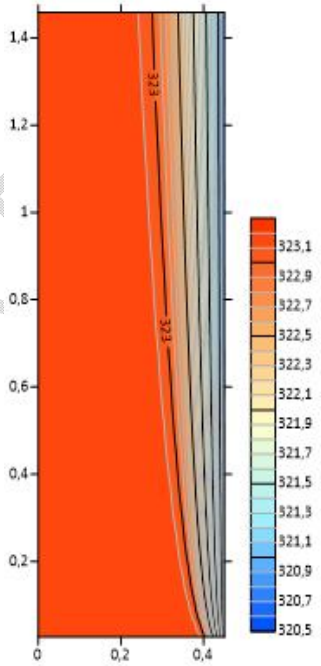

Fig.8. Thermal field, Re = 1000

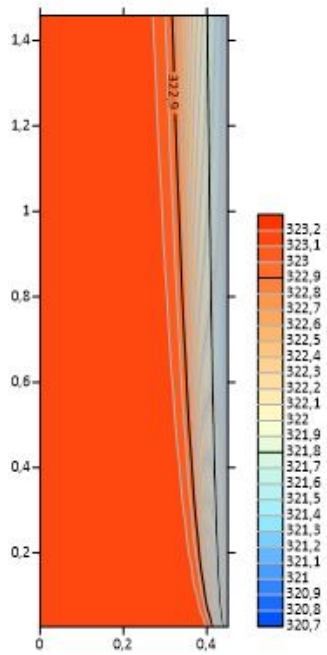

Fig.9. Thermal field, Re = 1500

3.5. INFLUENCE OF REYNOLDS NUMBER ON MASS FIELD

Figures (10-12) show mass field for three different Reynolds numbers (500, 1000 and 1500). The mass concentration iso-values show a distribution similar to that of the isotherms. The highest mass concentration values are found in the center of the channel. The similarity between mass and thermal distributions is explained by the Prandtl and Schmidt numbers, which are close for water vapor. The increase in Reynolds number is accompanied by the concentration of iso-concentration lines towards the walls. Indeed, the increase in inertial forces attenuates the mass boundary layer.

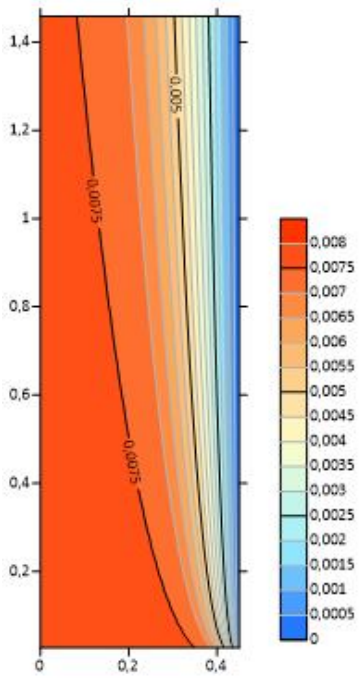

Fig. 10. Massfield, Re = 500

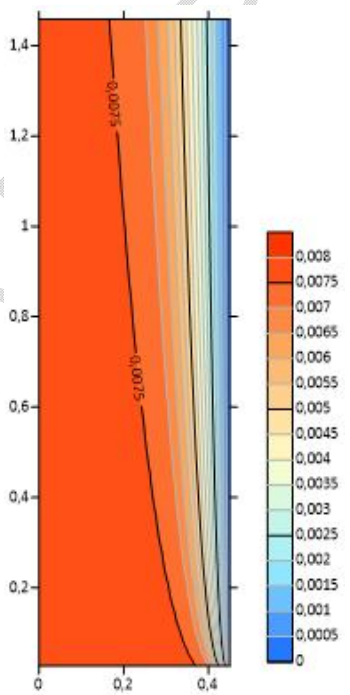

Fig. 11. Massfield, Re = 1000

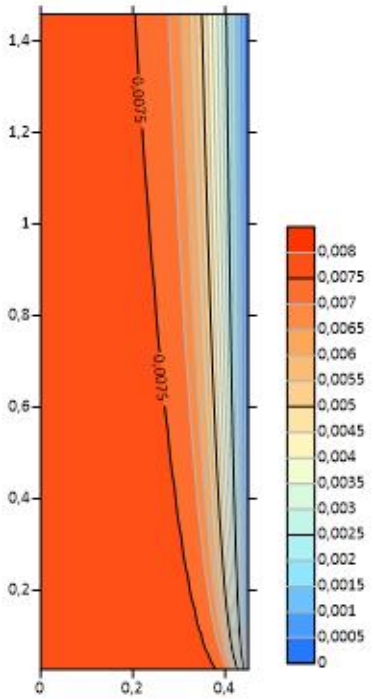

Fig. 12. Massfield, Re = 1500

3.6. REYNOLDS NUMBER INFLUENCE ON HEAT TRANSFER

Figures (13-14) show the evolution of the latent and sensitive Nusselt numbers along the channel as a function of Reynolds number.We note that the latent and sensitive Nusselt numbers show large values at the channel inlet and smaller values at the outlet. This is due to the steep thermal gradients at the leading edge of the channel. At the channel outlet, these gradients become small due to wall heating. We also note a gradual increase in these numbers as a function of Reynolds number. This is because increasing flow velocity enhances convective heat transfer, leading to an increase in latent and sensible heat transfer. As the latent heat of vaporization is high, latent-mode heat transfer is greater than sensible-mode heat transfer for the same inertial forces.

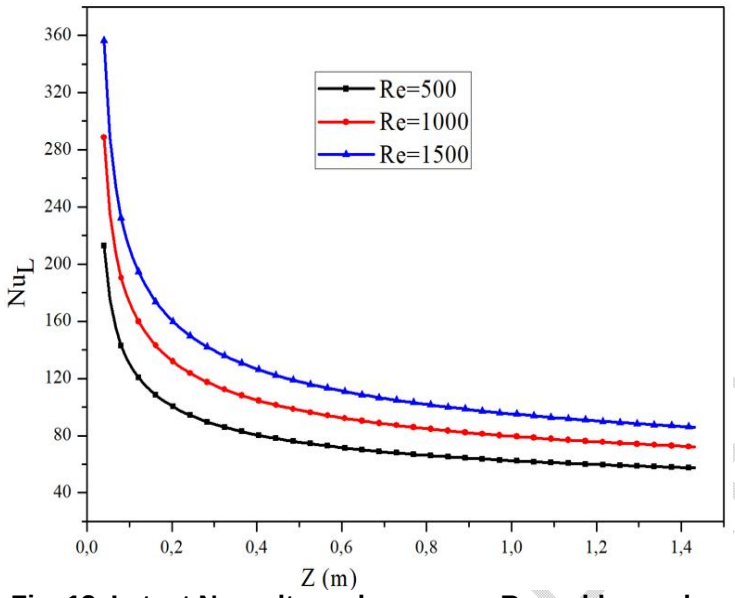

Fig. 13. Latent Nusselt number versus Reynolds number

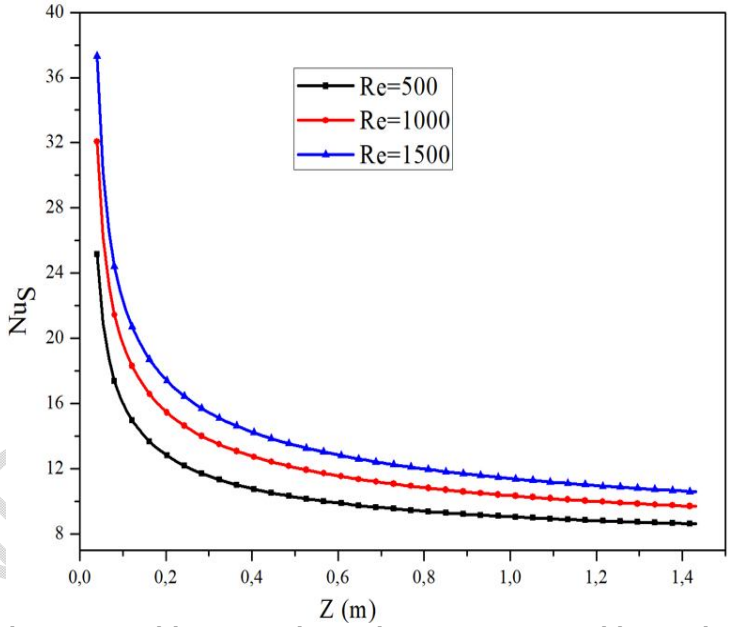

Fig. 14. Sensitive Nusselt number versus Reynolds number

4. CONCLUSION

In this work, we carried out a numerical study of coupled heat and mass transfer in a vertical channel with wet walls, whose heat exchange with the outside environment is governed by natural convection and radiation. Forced laminar flow was modeled by the Navier-Stokes equations and the flow conservation equation. The equation obtained were discretized using the finite volume method and then solved using the Thomas and Gauss algorithms. The effect of Reynolds number on heat and mass transfer has been studied in detail.The results indicate that an increase in Reynolds number leads to an increase in heat and mass

transfer. This increase is greatest at the leading edge of the channel. Latent heat transfer remains dominant throughout the channel.

NOMENCLATURES

A*: Dimensionless value
T: Temperature (K)
H: Channel height (m)
R: Channel radius (m)
V: Radial velocity ($m.s^{-1}$)
U: Axial velocity ($m.s^{-1}$)
t: Time (s)
P: Pressure ($N.m^{-2}$)
Cp:Thermal mass capacity ($JKg^{-1}.K^{-1}$)
Q:Flow rate ($m^3.s^{-1}$)
D:Diffusion coefficient ($m^2.s^{-1}$)
L: Latent heat ($J.Kg^{-1}$)
E: Thickness (m)
h:Heat transfer coefficient ($W.m^{-2}.K^{-1}$)
M: Molar mass ($Kg.mol^{-1}$)
Gr: Grashof number
Re: Reynolds number
Nu: Nusselt number
Sh: Sherwood number
Pr: Prandtl number
Sc: Schmidt number
g:Accelerating gravity ($m.s^{-2}$)
β:Thermal expansion coefficient (K^{-1})
ϑ:Kinematic viscosity ($m^2.s^{-1}$)
μ: Dynamic viscosity ($Kg.m^{-1}.s^{-1}$)
σ: Stefan Boltzmann's constant ($W.m^{-2}.K^{-4}$)
Dh: Hydraulic diameter (m)
$\dot{m}''$: Evaporated mass flow rate ($Kg.s^{-1}$)
λ: Thermal conductivity ($W.m^{-1}.K^{-1}$)
ρ: Density ($Kg.m^{-3}$)

REFERENCES

1. Oubella M, Feddaoui M, Mir R. Numerical study of heat and mass transfer during evaporation of a thin liquid film. Thermal Science. 2015; 19(5):1805–1819;DOI: 10.2298/TSCI130128145O.

2. Mechergui O. Numerical study of mass and heat transfers in natural convection in a channel: influence of the shape of the wall. Thesis University of Perpignan Via Domita; France 2017. French.

3. Raji A, Hasnaoui M. Correlations in mixed convection in ventilated cavities. General Thermal Review. 1998; 37:874–884. French.

4. Oulaid O, Benhamou B, Galanis N. Effect of the variability of thermo-physical properties on coupled heat and mass transfers in a vertical channel. 14th International Thermal Days. Tunisia 2009. French.

5. Boukadida N, Nasrallah SB. Mass and heat transfer during water evaporation in laminar flow inside a rectangular channel - validity of heat and mass transfer analogy. International Journal of Thermal Sciences. 2001; 40(1):67–81. DOI: 10.1016/S1290-0729(00)01181-9.

6. Helel D, Boukadida N. Heat and mass transfer in an unsaturated porous medium subjected to laminar forced convection. 13th International Thermal Days. France 2007. French.

7. Oulaid O, Benhamou B, Galanis N. Combined buoyancy effects of thermal and mass diffusion on laminar convection in a vertical isothermal channel. Computational Thermal Sciences. 2010; 2(2):125–138;DOI:10.1615/ComputThermalScien.v2.i2.30.

8. Lin TF, Chang JY, Yan WM. Analysis of combined buoyancy effects of thermal and mass diffusion on laminar forced convection heat transfer in a vertical tube. Journal of heat transfer. 1988; 110:337–344: DOI: 10.1115/1.3250489.

9. Yan W, Ting S, Soong C. Convective heat and mass transfer along an inclined heated plate with film evaporation. International journal of heat and mass transfer. 1995; 38(7):1261–1269; DOI: 0017-9310(94)00241-X.

10. Mezaache E, Daguenet M. Effects of inlet conditions on film evaporation along an inclined plate. Solar energy. 2004; 78:535–542; DOI: 10.1016/j.solener.2004.04.007.

11. Cherif AS, Jabrallah SB, Corriou JP, Belghith A. Intensification of the liquid film evaporation in a vertical channel. Desalination. 2010; 250(1):433–437. DOI: 10.1016/j.desal.2009.09.071.

12. Cherif AS, Kassim MA, Benhamou B, Harmand S, Corriou JP, Jabrallah SB. Experimental and numerical study of mixed convection heat and mass transfer in a vertical channel with film evaporation. International Journal of Thermal Sciences. 2011;50(6):942–953. DOI: 10.1016/j.ijthermalsci.2011.01.002.

13. Turki S, Abbassi H, Nasrallah SB. Two-dimensional laminar fluid flow and heat transfer in a channel with a built-in heated square cylinder. International Journal of Thermal Sciences. 2003; 42:1105–1113, 2003. DOI: 10.1016/S1290-0729(03)00091-7.

14. Zermane S, Boudebous S, Boulkroune N. Numerical study of laminar mixed convection in ventilated cavities. Science & Technology.2005;23:34–44.

15. Diallo DM. Mathematical modeling and numerical simulation of hydrodynamics: case of flooding downstream of the Diama dam. Thesis; University of Franche-Comté, 2010. France. French.

16. Feddaoui M, Mir A, Belahmidi E. Cocurrent turbulent mixed convection heat and mass transfer in falling film of water inside a vertical heated tube," International Journal of Heat and Mass Transfer.2023;46(18):3497–3509. DOI: 10.1016/S0017-9310(03)00129-7.

17. Eckert ER, Drake R. Analysis of heat and mass transfer. 1972. New York.

18. Sacadura JF. Thermal transfers: initiation and deepening. 2015;625–691. ISBN: 978-2-7430-1993-8. Lavoisire. Paris. French.

19. Oulaid O. Coupled transfer of heat and mass by mixed convection with phase change in a channel. Thesis 2010. University of Sherbrooke, Canada. French.